ACTA ABP BIOCHIMICA POLONICA

Epub: No 2620
Vol. 65, 2018
https://doi.org/10.18388/abp.2018_2620

Regular paper

Molecular characterization of central cytoplasmic loop in *Aspergillus nidulans* AstA transporter

Sebastian Piłsyk[1]✉, Marzena Sieńko[1], Jerzy Brzywczy[1], Maciej P. Golan[2], Urszula Perlińska-Lenart[1] and Joanna S. Kruszewska[1]

[1]Institute of Biochemistry and Biophysics, Polish Academy of Sciences, Warsaw, Poland; [2]Opta – Tech Co. Ltd., Warsaw, Poland

AstA (alternative sulfate transporter) belongs to a large, but poorly characterized, Dal5 family of allantoate permeases of the Major Facilitator Superfamily. The *astA* gene has been cloned from an IAM 2006 Japanese strain of *Aspergillus nidulans* by complementation of a sulfate permease-deficient mutant. In this study we show that conserved lysine residues in Central Cytoplasmic Loop (CCL) of the AstA protein may participate in anion selectivity, and control kinetic properties of the AstA transporter. A three-dimensional model containing four clustered lysine residues was created, showing a novel substrate-interacting structure in Major Facilitator Superfamily transporters. The assimilation constant (K_τ) of wild type AstA protein is 85 μM, while V_{max}/mg of DW of AstA is twice that of the main sulfate transporter SB per mg of dry weight (DW) of mycelium (1.53 *vs*. 0.85 nmol/min, respectively). Amino acid substitutions in CCL did not abolish sulfate uptake, but affected its kinetic parameters. Mutants affected in the lysine residues forming the postulated sulfate-interacting pocket in AstA were able to grow and uptake sulfate, indicating that CCL is not crucial for sulfate transportation. However, these mutants exhibited altered values of K_τ and V_{max}, suggesting that CCL is involved in control of the transporter activity.

Key words: *Aspergillus nidulans*, sulfate permease, alternative sulfate transporter, AstA, intracellular loop, mutagenesis

Received: 28 May, 2018; revised: 03 July, 2018; accepted: 20 September, 2018; available on-line: 14 November, 2018

✉e-mail: Seba@ibb.waw.pl

Abbreviations: CCL, central cytoplasmic loop; MFS, Major Facilitator Superfamily; SMR, sulfur metabolite repression; TM, transmembrane; K_τ, assimilation constant; PCR, polymerase chain reaction; OE-PCR, overlap extension polymerase chain reaction

INTRODUCTION

Sulfate is taken up and utilized for the synthesis of organic sulfur compounds by bacteria, fungi and plants. In eukaryotes, sulfate uptake is carried out by sulfate permeases from the SulP family (Kertesz 2001; Loughlin *et al*., 2002; Piłsyk & Paszewski 2009; Alper & Sharma 2013). These proteins are assigned to the TC 2.A.53 class, according to the Transporter Classification (TC) system. In *Aspergillus nidulans* the main sulfate permease is encoded by the *sB* gene, however, an alternative sulfate transporter (AstA) is also functional in some *A. nidulans* strains. The *astA* gene has been cloned earlier from a genomic library of the Japanese IAM 2006 strain, as a suppressor complementing sulfate permease-deficiency of the *sB* mutant (Piłsyk *et al*., 2007). The *astA* gene is regulated at the transcriptional level by sulfur metabolite repression (SMR), being derepressed under sulfur limitation conditions. In the reference *A. nidulans* strains of Glasgow origin *astA* is non-functional, thus, SB is the only sulfate permease in these strains. Recently, it was shown that AstA transports also sulfite and choline sulfate (Holt *et al*., 2017). Orthologues of *astA* occur frequently in evolutionarily distant fungi belonging to the *Dikarya* phylum with often common feature of plant or animal pathogenicity. An *astA* orthologue identified from pathogenic *Fusarium sambucinum* fungus was found to be derepressed during potato tuber infection, where the AstA protein may efficiently take up sulfate (Piłsyk *et al*., 2015).

The *A. nidulans* AstA protein (GenBank® accession number ABA28286) is a member of the poorly characterized Dal5 allantoate permease family belonging to the Major Facilitator Superfamily (MFS, TC 2.A.1). The MFS transporters are localized in the cell membrane or in organellar membranes facilitating the transport of various substrates (ions, sugars, drugs, neurotransmitters, amino acids, or peptides). Contrary to ATP-dependent SulP family of sulfate permeases (Tweedie & Segel 1970, Woodin & Wang 1989), three different mechanisms of transport *via* MFS transporters are distinguished: uniporters transporting one type of substrate and energized by its gradient, symporters translocating simultaneously two or more substrates and drawing energy from the electrochemical gradient of one of them, and antiporters transporting two or more substrates in opposite directions (Law *et al*., 2008; Iancu *et al*., 2013; Ethayathulla *et al*., 2014; Patron *et al*., 2014). The AstA transporter can uptake sulfate in proton symport-driven energy (Holt *et al*., 2017). Until now, only one report presented experimental evidence for ATP-independence of MFS - the gene encoding Hxt13p hexose transporter was cloned while screening the yeast genomic library for resistance to antifungal drug miltefosine (Biswas *et al*., 2013). The authors have shown that Hxt13p acts as an ATP-independent efflux pump for miltefosine. On the other hand, it was shown that GLUT1 glucose transporter in human erythrocytes binds ATP, which triggers significant conformational changes in GLUT1 that lead to its inactivation (Blodgett *et al*., 2007). In this case ATP serves as low molecular weight effector rather than energy source.

Crystal structures of bacterial MFS transporters (FucP, LacY, GlpT, EmrD) have revealed the presence of 12 transmembrane (TM) alpha helices. These helices are clustered in the N- and C-terminal domains, each comprising six helices (Fig. 1) (Abramson *et al*., 2003; Lemieux *et al*., 2004; Yin *et al*., 2006; Dang *et al*., 2010). A similar structure of 12 TM helices has also been identified in another MFS phosphate transporter, the PiPT protein of the *Piriformospora indica* fungus (Pedersen *et al*.,

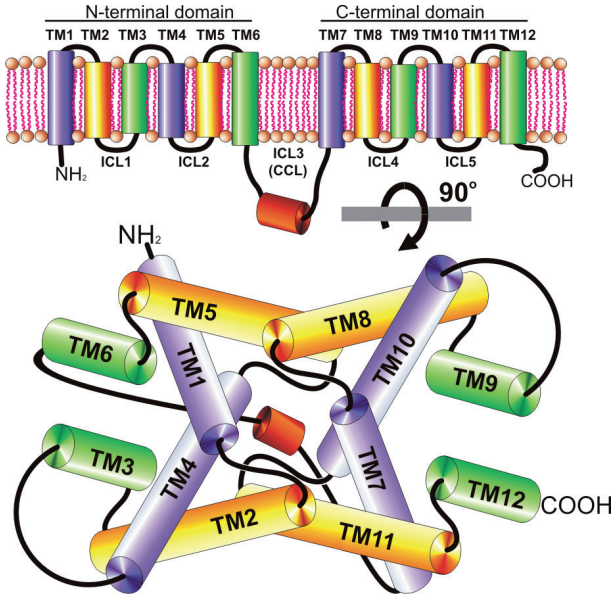

Figure 1. The predicted transmembrane topology of MFS transporters (upper) and their general 3D model (lower), based on known crystal structures (PDB IDs: 3O7Q, 2V8N, 1PW4, 2GFP, 4J05).

2013). The substrate-binding residues are found in various TM helices: TM5 in the *Candida albicans* Mdr1p protein (Pasrija *et al.*, 2007), TM7 in human GLUT-1 (Kasahara *et al.*, 2009), TM1, TM5 and TM7 in *E. coli* GlpT and FucP (Lemieux *et al.*, 2004; Dang *et al.*, 2010), and TM5, TM 7, TM10 and TM11 in *E. coli* XylE (Sun *et al.*, 2012). Between the N- and C-terminal domains of all MFS proteins, a third domain is present, called the Central Cytoplasmic Loop (CCL).

Substrate uptake mechanism of MFS transporters involves a rocker-switch type of movement, followed by transient formation and breakage of a salt bridge between positively and negatively charged amino acids located opposite in the apical surface of the TM helices (Law *et al.*, 2008). Thus, CCL transiently forms a latch-like structure in the outward-facing open conformation, while in the inward-facing open conformation, it unfolds into a partially disordered chain and swings away from the substrate translocation pathway (Wisedchaisri *et al.*, 2014). Additionally, CCL acts as a constraint for movement of the N- and C-terminal domains and permits a relatively large interdomain movement, which has implications for the substrate translocation mechanism (Law *et al.*, 2008). It has also been shown that CCL is critical for efficient substrate transport by the *C. albicans* Mdr1 multidrug transporter (Mandal *et al.*, 2012) and likely participates in formation of a substrate translocation pore.

In this study, we demonstrate that CCL of the *A. nidulans* AstA protein controls sulfate transport. The role of four conserved lysine residues in the *A. nidulans* AstA protein was analyzed using site directed mutagenesis. Interestingly, four single amino acid substitutions (K_{260}A, K_{263}A, K_{263}L and K_{264}L), introduced in the substrate-interacting region of AstA, led to more selective uptake of sulfate compared to selenate.

MATERIALS AND METHODS

Strains and media. The *Aspergillus nidulans* strains from our collection, carrying standard markers (Clutterbuck 1994; Martinelli 1994), together with the *Escherichia coli* strain used in this study, are listed in Table 1. The M111 strain, derived from Glasgow wild-type, bearing the *sB43* mutation complemented with the *sB* gene and carrying a non-functional *astA* gene, was used as the *A. nidulans* reference strain.

Growth conditions. The following media (solid and liquid) were used: complete medium (CM) (Cove, 1966) for protoplasts or DNA isolation, minimal medium (MM) or minimal sulfur free medium (MM-S) (Lukaszkiewicz & Paszewski 1976), the latter supplemented either with sulfate (1 mM, inorganic sulfur) or L-methionine (0.1 mM, organic sulfur). The minimal media were also supplemented according to the auxotrophic requirements of the cultured strain. Liquid cultures were grown at 37°C for 16 hours in a rotary shaker (200 rpm). The culture doubling times were calculated using the Doubling Time Computing web page (Roth 2006). *Escherichia coli* was grown in the standard LB medium supplemented with antibiotics as described before (Sambrook *et al.*, 1989).

Table 1. Growth rates of AstA transformants on solid and liquid MM-S media supplemented with 1 mM sulfate, transportation constant and maximum velocity of sulfate transport to mycelia expressing SB or AstA variants. The results are average values from at least three biological replicates.

Transformant	Growth on solid medium [mm/h]	Doubling time in liquid medium [h]	Sulfate uptake [nmol/min/mg DW] av.	K_τ [μmol]	V_{max} [nmol/min/mg DW]
TRSBWT	0.23	6.70	1.50	108	0.85
TRAstAWT	0.21	5.44	0.74	85	1.53
TRAstAK_{260}A	0.25	5.16	1.02	25	1.15
TRAstAK_{260}L	0.21	3.81	1.12	36	1.47
TRAstAK_{262}A	0.23	5.53	0.79	77	1.37
TRAstAK_{262}L	0.19	7.98	0.62	72	0.65
TRAstAK_{263}A	0.23	4.15	0.82	49	0.95
TRAstAK_{263}L	0.21	5.01	1.27	76	2.79
TRAstAK_{264}A	0.19	5.68	1.22	50	1.05
TRAstAK_{264}L	0.21	3.46	1.33	37	3.70
TRAstA$K_{260\text{-}264}$A	0.18	2.86	0.89	137	1.36

Nucleic acids manipulations, plasmid construction and mutagenesis. The plasmids used in this study are listed in Table 1. Plasmids were propagated and isolated according to the standard procedures (Sambrook *et al*., 1989). *A. nidulans* DNA was isolated using a salting out method. The frozen mycelia were disrupted by grinding in liquid nitrogen, followed by immediate suspension in warm STEN buffer (1% SDS, 100 mM Tris pH 7.5, 50 mM EDTA pH 8, 100 mM NaCl) (Sambrook *et al*., 1989). Polymerase chain reactions (PCR) were performed in a Techne Thermocycler. DNA was sequenced, and primers were synthesized by the DNA Sequencing and Oligonucleotide Synthesis Laboratory, Institute of Biochemistry and Biophysics, PAS. The sequences of the primers used are provided in supplementary Table S1. The kPMS11-52 plasmid carrying the wild-type *astA* gene (Pilsyk *et al*., 2007) was modified by an insertion of the *Neurospora crassa pyr-4* selection cassette into the PvuII restriction site yielding the kPMS11-524 plasmid. The latter could be selected by uridine prototrophy and was used for construction of a series of plasmids bearing the mutated *astA* alleles. Selected lysine residues were changed to alanine or leucine using Overlap Extension PCR (OE-PCR) with Pfu polymerase (Thermo Scientific). Obtained PCR products were cleaved with the SnaBI and MunI restriction enzymes (Thermo Scientific) and ligated into the kPMS11-524 vector digested with the SnaBI and MunI restriction enzymes to replace the wild type *astA*. These mutations were verified by DNA sequencing and introduced into the *A. nidulans* sulfate permease-deficient M111 strain bearing the *sB43* mutation (Table 1).

A 3.3 kb PstI fragment of the non-functional *ΨastA* gene was excised from the kPB6-7 plasmid (Pilsyk *et al*. 2007) and inserted into kPG23B yielding kPG23ΨastA plasmid. For reconstitution of the missing functional TM11-TM12 domains in ΨAstA, a 3.2 kb SpeI fragment from kPMS11-524 plasmid (last 586 nucleotides of *astA* 3' ORF encoding TM11-TM12 together with *N. crassa pyr-4* selection cassette) was ligated between SpeI restriction sites of kPB6-7 plasmid, yielding kPB611-12.

The Green Fluorescent Protein-labeled *astA* allele was constructed with OE-PCR of PCR-generated GFP with PCR-generated *astA* wild type allele using overlapping primers. The hybrid product was initially cloned into pGEM®-T Easy vector (Promega), then excised with MunI-Van91I, and inserted into MunI-Van91I sites of kPMS11-524, yielding the kPMS11-5243 plasmid. Similarly, the same MunI-Van91I fragment was introduced into a series of kPMS11-524 derivatives bearing the mutated *astA* alleles.

Transformation of *A. nidulans* strains. The mycelia for transformation were collected by filtration, washed with 0.6 M KCl and suspended in 0.6 M KCl buffered with 10 mM potassium phosphate pH 6.5 and containing the following lytic enzymes: 15–20 mg/ml of Glucanex® (Novozymes), 2 mg/ml of Driselase® (Sigma-Aldrich) and 1 mg/ml of snail acetone powder (Sigma-Aldrich). The protoplasts were prepared and transformed using the PEG method (Kuwano *et al*., 2008). To increase transformation efficiency, 5 μg of the HELp helper plasmid (Gems & Clutterbuck 1993) was added. Transformants were selected for uracil prototrophy on MM-S medium supplemented with 2 mM sulfate and 1.2 M sorbitol.

Sulfate uptake assay. The sulfate uptake analysis was performed as described previously (Pilsyk *et al*., 2015) using 0.1 mM methionine – supplemented MM-S for mycelia growing under derepressing conditions. Ten ml aliquots were taken after 2, 3, 5, 10, 15 and 20 min of incubation, and the sulfate transport rates [nmol/mg dry weight] were calculated based on at least three measurements taken at different times.

For the estimation of the assimilation constant (K_t), a cold sulfate was added to the final concentrations of 0.166, 0.2, 0.25, 0.33, 0.5 and 1 mM, and incubations were carried out for 1 h. Mycelia were treated as above and the initial rate of transport [nmol/min/mg dry weight] was calculated for each concentration of the sulfate, based on at least four measurements. These data were rendered as Hanes-Woolf plots, and linear regression was used for calculation of V_{max} from the slope, and K_t from the ordinate axis intercept.

Confocal microscopy. The mycelia for microscopic observations were grown in liquid MM-S medium supplemented with 0.1 mM methionine (derepressing conditions) for 18 h at 37°C in a rotary shaker (200 rpm). The mycelia were harvested by filtration, suspended in fresh MM-S medium supplemented with 1 mM sulfate and kept at 37°C in a rotary shaker (200 rpm). The mycelial samples were collected at time of the medium shift (t 0) and 5 h after the shift, and examined under a Nikon Eclipse TE2000-E inverted microscope (Nikon, Tokyo, Japan).

Membrane protein isolation. For protein isolation, the mycelia were grown as above (*Confocal microscopy*), and the samples were harvested just before and 5 h after a shift to repressing conditions. Next, the collected samples were ground in TM isolation buffer (30 mM Tris-HCl pH 7.4, 50 mM EDTA pH 8, 1% sorbitol, 0.05% Tween-20, 200 mM NaCl, 20 mM dithiothreitol, 1 mM PMSF, protease inhibitors Complete™-Roche), and the homogenate was centrifuged at 4000×*g* for 10 min. The supernatants were centrifuged for 1 h at 50 000×*g* and the pelleted membrane fractions were used for Western dot-blots.

Immunodetection of AstA-GFP protein. Membrane proteins suspended in TM isolation buffer were subjected to the Immobilon P membrane (Milipore), and AstA-GFP protein was detected with rabbit anti-αGFP polyclonal antibodies (Life Technologies). Polyclonal rabbit antibodies raised against entire yeast Pma1p protein were used as an internal reference standard. Anti-rabbit IgG secondary antibodies conjugated to alkaline phosphatase (Sigma-Aldrich) were then applied as secondary antibodies. After washing, dots were visualized using BCIP/NBT (Promega).

Protein quantification. Protein concentration was estimated according to Lowry *et al*. (1951).

Bioinformatics. Multiple alignments of protein sequences were generated using the MUSCLE software (URL: http://www.drive5.com/muscle/) (Edgar, 2004). Homology searches of the GenBank database (release 95.0) were carried out using the BLAST program (Altschul & Lipman, 1990). Transmembrane topology was predicted basing on four independent algorithms: the PredictProtein server ver. 10.20.04 (https://www.predictprotein.org/) (Rost *et al*., 2004), TMpred (https://embnet.vital-it.ch/software/TMPRED_form.html)(Hofmann & Stoffel 1993), PSIPRED (http://bioinf.cs.ucl.ac.uk/psipred/)(Buchan *et al*., 2013) and SMART (http://smart.embl-heidelberg.de/) (Letunic & Bork 2017). Modeling of 3D structure and ligand binding were performed with the I-TASSER metaserver (Zhang 2008; Roy *et al*., 2010; Roy *et al*., 2012). The image of CCL was created with RasMol (Sayle & Milner-White, 1995).

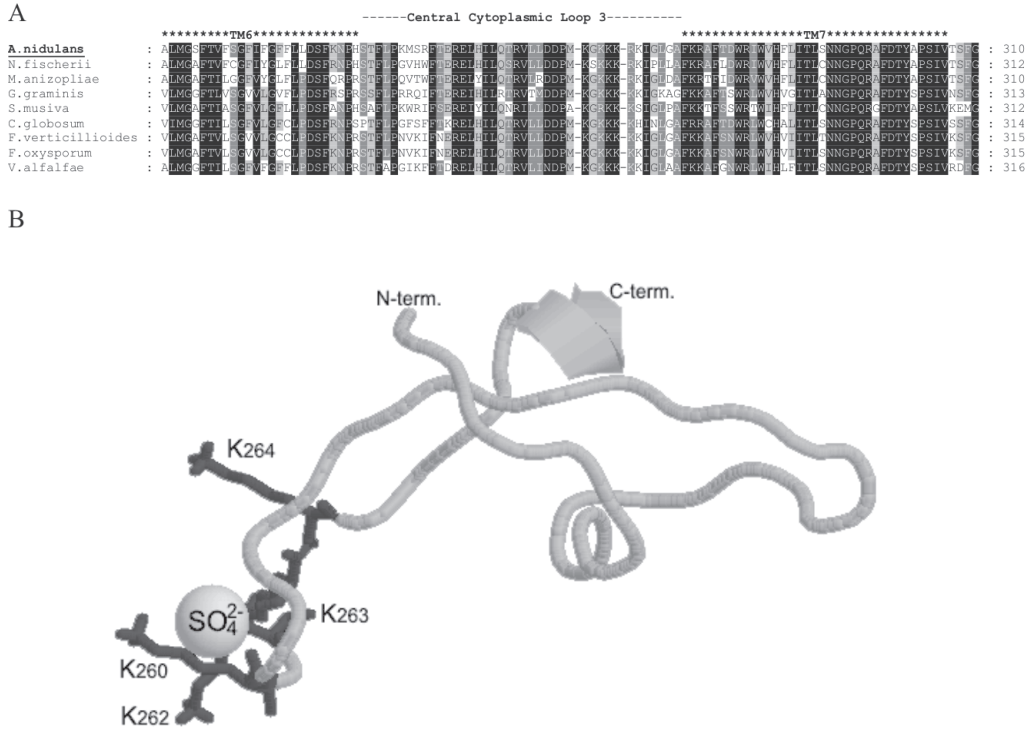

Figure 2. (A) Alignment of the *Aspergillus nidulans* AstA sequence with its orthologues from the *Pezizomycotina* subphylum. Conserved residues are dark-shaded. The Central Cytoplasmic Loop is located between transmembrane helices TM6 and TM7, which are marked with asterisks above the alignment. The highly conserved motif comprising four lysine residues is boxed. Access numbers of sequences are indicated in parentheses: *Aspergillus nidulans* (ABA28286), *Neosartorya fischerii* (NFIA_049850), *Metarhizium anisopliae* (MAA_07643), *Gaeumannomyces graminis* (GGTG_08696), *Septoria musiva* (SEPMUDRAFT_60592), *Chaetomium globosum* (CHGG_02116), *Fusarium verticillioides* (FVEG_12081), *F. oxysporum* (FOYG_01075) and *Verticillium alfalfae* (VDBG_07944).
(B) Structure of the Central Cytoplasmic Loop predicted by I-TASSER. Putative substrate-binding pocket comprises four lysine residues, which are marked in dark-grey and signed.

RESULTS

Verification of astA allele functionality

Our previous studies showed that sB mutants in A. nidulans could be complemented by the astA gene only when it was derived from the Japanese IAM2006 strain. Numerous attempts to complement the auxotrophic phenotype of sB mutants by a copy of astA derived from a reference wild-type strain of Glasgow origin, have failed (Piłsyk *et al*., 2007). Northern blot analysis of the astA expression in the reference strain showed no detectable signal. Moreover, comparison of the nucleotide sequences of astA ORFs in the Japanese and Glasgow strains suggested numerous mutations and deletions in the latter (Piłsyk *et al*., 2007), including lack of 187bp sequence putatively encoding TM11 and TM12 (Suppl. Fig. S1 at www.actabp.pl). These mutations might abolish the function of the putative AstA protein in the reference strain. Hence, we concluded that this allele exists as a pseudogene (Ψ astA). However, RNA-seq results allowed for a distinction of transcriptional unit in AspGD, and transcriptomic data indicate that the astA locus (AN10387) in the reference strain is transcribed (Cerqueira *et al*., 2014; Sieńko *et al*., 2014).

To verify functionality of the Ψ astA gene, we generated two constructs bearing selectable N. crassa pyr-4 cassette and the Ψ astA gene or Ψ astA fused with functional sequence coding for TM11-TM12 from the Japanese astA allele. However, transformation of sB mutant with these constructs did not restore sulfate prototrophy (see: Suppl. Fig. S1 at www.actabp.pl). Thus, the lack of TM11 and TM12 helices was not the only reason for abolishing function of the astA gene in strains of Glasgow origin, but the other mutations of the astA ORF present in theses strains were sufficient to abolish protein activity. Hence, in further studies a copy of the astA gene derived from the Japanese IAM2006 strain was used as a reference.

***In silico* analysis of the Central Cytoplasmic Loop**. A predicted topology of the *A. nidulans* AstA transporter revealed twelve transmembrane domains and a centrally located CCL (Fig. 1), the latter domain containing four lysine residues clustered into a tight bundle located in the middle of CCL – K_{260}, K_{262}, K_{263} and K_{264}. These four lysine residues, together with the fifth basic amino acid (arginine or lysine), are conserved in AstA orthologs from various fungal pathogens (Fig. 2A). We previously suggested that the positively charged CCL of AstA could be responsible for interaction with a negatively charged sulfate anion during translocation (Piłsyk *et al*., 2007). The AstA region from D_{225} through A_{275} was modeled using the I-TASSER meta-server (Zhang, 2008; Roy *et al*., 2010; 2012) (Fig. 2B). Five similar models of the AstA CCL bound with sulfate were obtained, and the highest-scoring one (Fig. 2B) was used in further studies. This model exhibits a small ligand-binding region comprising amino acids 260 through 264 and resembling the calcium-binding pocket of human frequenin (PDB ID: 1G8I, Bourne *et al*., 2001). The predicted sulfate-interacting pocket contains the four conserved lysine residues (K_{260}, K_{262}, K_{263} and K_{264}, see Fig. 2B), therefore, it seems likely that these lysine residues directly interact with the sulfate.

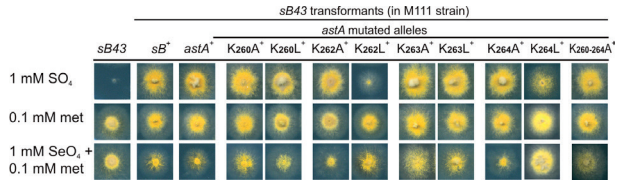

Figure 3. The growth of *A. nidulans sB43* mutant transformed with various *astA* alleles.
Solid minimal sulfur-free medium (MM-S) was supplemented with 1 mM sulfate, 0.25 mM methionine or 0.25 mM methionine with 1 mM selenate. The sulfate permease-deficient recipient strain (*sB43*) and transformants with the wild type *sB* or *astA* gene are included for comparison.

Central Cytoplasmic Loop mutants can grow. To check whether the lysine residues forming the predicted sulfate-interacting pocket (K_{260}, K_{262}, K_{263} and K_{264}) take part in sulfate transport, they were replaced individually with alanine or leucine, and additionally, a quadruple mutant with all four lysine residues changed to alanine was constructed. Small alanine residues are preferentially chosen as a substitution in site-directed mutagenesis, however, substitutions of lysine with leucine are also tested because of comparable size of these amino acids. Altogether, nine mutated *astA* alleles were generated using site-directed mutagenesis (Table 1). The functionality of the mutated *astA* alleles was tested by transformation of the *A. nidulans* M111 recipient strain, which bears non-functional *astA* gene and the *sB43* mutation, and is hence unable to grow on sulfate as the sole sulfur source (Arst 1968; Pilsyk *et al.*, 2007).

The obtained transformants were named by combining the TR letters denoting a transformant with the name of the modified protein and the amino acid substitution. Wild type alleles of *astA* and *sB* were also introduced into the M111 recipient strain, yielding the TRAstAWT and TRSBWT transformants, respectively (Table 1).

Almost all the tested *astA* alleles complemented the *sB43* mutation, rendering the transformants able to grow on sulfate, both on solid and in liquid minimal media (Fig. 3, Table 1). The TRAstAK$_{262}$L mutant grew poorly after 48 h on solid minimal medium, however, after longer incubation time it exhibited growth rate comparable to that of the wild type TRAstAWT.

A. nidulans strains bearing wild type *sB* are sensitive to selenate, a toxic analogue of sulfate, under derepressing conditions (0.1 mM methionine), opposite to sulfate permease-deficient strains (e.g., *sB43* mutants), which are resistant (Pilsyk *et al.*, 2007). In our study, when compared to wild 1type AstA, the K_{262}A or K_{264}A substitutions hardly affected growth in the presence of selenate, while the resistance to selenate of the K_{260}A, K_{263}A, K_{263}L and K_{264}L mutants was increased substantially, so that they could grow on MM-S medium containing 1 mM selenate (Fig. 3) even under derepressing conditions (0.1 mM methionine).

Central Cytoplasmic Loop mutants can take up sulfate

Sulfate uptake was measured in transformants of the M111 strain bearing the *sB43* mutation and various mutated *astA* alleles (Table 1), and compared with the TRAstAWT and TRSBWT strains serving as positive controls. The SB transporter in TRSBWT was more effective in sulfate uptake than the AstA mutants or wild type AstA (Fig. 4, Table 1). The K_{262}A, K_{263}A and $K_{260\text{-}264}$A mutations did not affect the uptake of sulfate significantly, while the K_{260}A, K_{260}L, K_{263}L, K_{264}A and K_{264}L mutations

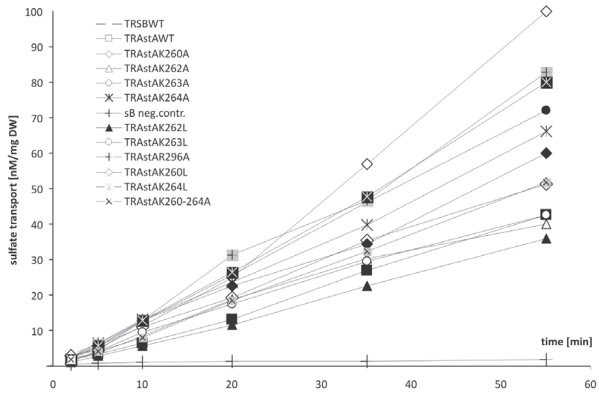

Figure 4. The sulfate uptake by transformants measured as influx of $^{35}SO_4^{2-}$.
The mycelia of the *sB43* mutant (negative control) and its transformants: with the *sB* gene (wild type sulfate permease, positive control), the *astA* gene (wild type AstA transporter) or mutated *astA* alleles, were grown overnight at 37°C in MM-S medium containing 0.1 mM methionine as a derepressing source of sulfur. Radioactive 1 mM sulfate was added, and aliquots of the mycelia were collected at the times indicated.

increased the uptake by 38, 51, 71.6, 64.9 and 79.7%, respectively, compared to TRAstAWT (Fig. 4, Table 1). K_{262}L decreased sulfate uptake by 16%. Altogether, the mutations affecting individual lysine residues in CCL did not abolish the sulfate uptake, moreover, most of the tested mutations led to even faster sulfate transport.

Mutations in Central Cytoplasmic Loop affect kinetics of sulfate uptake

Since the mutations affecting CCL did not impair sulfate uptake, it seemed possible that CCL could control its kinetics. Therefore, the effects of these mutations on the kinetic parameters of AstA were next studied. The K_t values determined for wild type AstA and the main sulfate permease SB were 85 μM and 108 μM, respectively (Fig. 5, Table 1). Each of the four substitutions of a single lysine with alanine or leucine decreased the K_t, with the most pronounced decrease observed in transformants bearing the K_{260}A, K_{260}L and K_{264}L mutations, by 70.6, 57.6 and 56.4%, respectively (Table 1). Conversely, the quadruple substitution of the four lysine residues in CCL with alanine led to an increase of the K_t by almost 40%.

The V_{max} for wild type transporters was 0.85 (nmol/min) for SB, and twice as much (1.53) for AstA, measured per mg of dry weight (DW) of mycelium (Fig. 5, Table 1). Each substitution of lysine with alanine in AstA led to a lowering of V_{max} – a high decrease (by 48%) was observed in the K_{263}A mutant. Meanwhile, K_{262}L substitution led to the strongest decrease of transport velocity (by 57.5%), while two other mutants (TRAstAK$_{263}$L and TRAstAK$_{264}$L) had significantly increased velocity of transportation (by 82.4 and 142%, respectively). A single K_{260}L mutation, or a quadruple substitution of all four lysine residues in CCL with alanine, did not affect V_{max} significantly. In summary, the substitutions of the lysine residues located in CCL resulted in various changes of both V_{max} and K_t, suggesting that these residues are important for controlling activity of the AstA transporter. The highest increase of K_t (up to 161%) was observed in the quadruple TRAstAK$_{260\text{-}264}$A mutant, in which all four lysine residues in CCL were replaced with alanine.

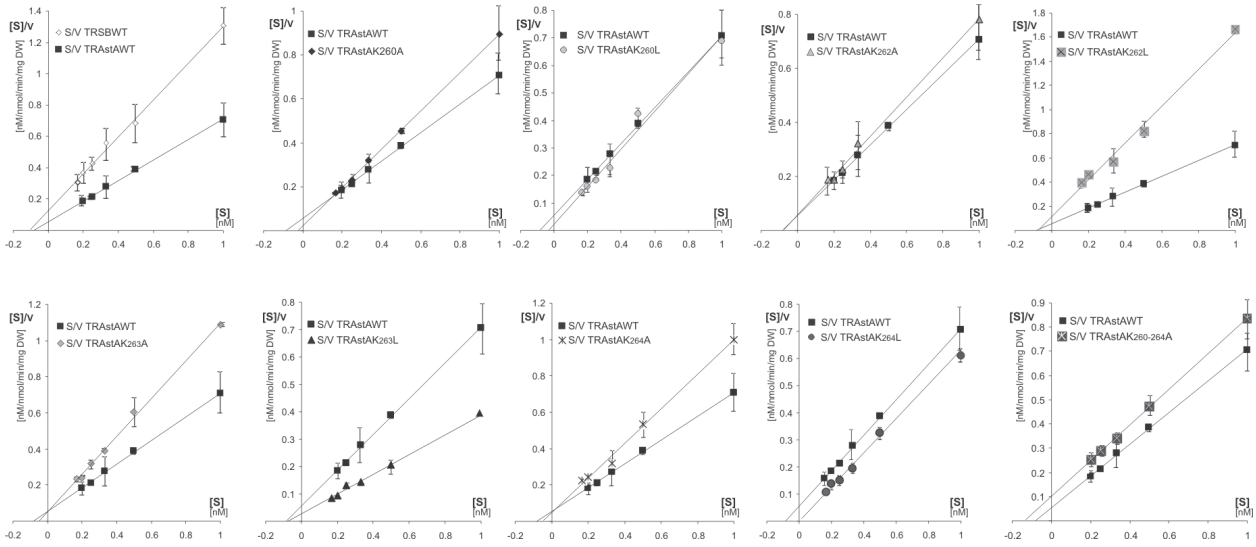

Figure 5. Kinetics of the sulfate uptake by mycelia expressing mutated AstA variants compared to the wild type SB and AstA transporters.
Sulfate was added at concentrations ranging from 0.166 to 1 mM and sulfate uptake was measured as described in Materials and Methods.

AstA protein localization and stability

To verify if the mutated AstA proteins were properly located in the cell membrane during the kinetic studies, each mutated AstA variant fused with GFP was expressed in the M111 recipient strain and examined under microscope. In all the transformants, both the GFP-tagged wild type AstA protein and its mutated variants were correctly located in the cytoplasmic membrane, both before and after the shift to repressing conditions (Suppl. Fig. S2A at www.actabp.pl). Additionally, the amount of AstA-GFP or its mutated variants was verified by Western dot-blot analysis (Suppl. Fig. S2B at www.actabp.pl), indicating that the AstA protein and its mutant versions were stable in the applied experimental conditions.

Sulfate uptake by AstA is ATP-independent, in contrast to SB (SulP) permease

In order to study AstA transport mechanism, we compared the effect of 100 μM sodium azide on the radioactive sulfate uptake by the TRSBWT or TRAstAWT strains (Fig. 6). Sulfate uptake by the SB permease was significantly decreased by azide while AstA was resistant to the azide treatment. Since azide inhibits ATP-synthase (Bowler *et al.*, 2006), it leads to a decreased intracellular ATP level. Thus, azide-insensitive transport exhibited by the AstA transformant indicates an ATP-independent transport mechanism, contrary to the SB sulfate permease, which is ATP-dependent (Fig. 6 and earlier published results by Tweedie & Segel 1970; Woodin & Wang, 1989).

DISCUSSION

Alternative sulfate transporter AstA, a member of the MFS transporters, is found in some fungi, particularly frequently in pathogenic species. Numerous mutations present in the *astA* locus (AN10387) in the *A. nidulans* reference strain abolish its functionality, as it was postulated earlier (Piłsyk *et al.*, 2007) and confirmed in this study. Despite of detectable transcription of the *ΨastA* locus (Cerqueira *et al.*, 2014, Sieńko *et al.*, 2014), the protein product is either not produced or non-functional. We showed that truncated *ΨastA* was unable to complement the sulfate permease-deficient mutants, even when its ORF was reconstituted with a missing 3' sequence encoding the last two TM helices 11 and 12. This result supports our earlier conclusion that the *astA* allele derived from the Japanese IAM2006 strain is functional, while *A. nidulans* strains of Glasgow origin contain pseudogene sequences.

Structural studies of various MFS transporters have shown the presence of two transmembrane domains, each one comprising six membrane-spanning helices. The two domains are connected by the central cytoplasmic loop (CCL) (Fig. 1), predictably localized in the way of the transported substrate (Law *et al.*, 2008).

Looking for the role of CCL in AstA, we focused on a highly conserved motif of four lysine residues present in AstA orthologs from various fungi (Fig. 2A). These positively charged residues seemed to interact with a negatively charged sulfate ion during translocation, and this assumption was confirmed by the predicted structure of CCL bound with sulfate. Therefore, the role of

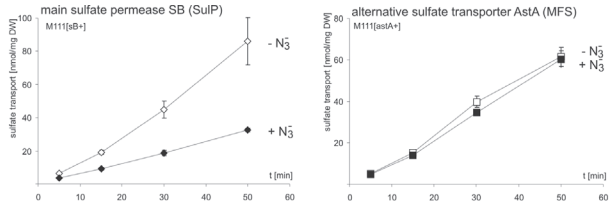

Figure 6. Sulfate uptake by the strains over-expressing SB (A) or AstA (B).
The results are average values from at least four biological replicates. ^{35}S-labeled sulfate was added to the mycelia grown in liquid media in the absence or presence of 100 μM azide, as indicated in figure legend. The mycelia could take up $^{35}SO_4^{2-}$ as described in Materials and Methods. Samples were collected at four time points and intracellular [^{35}S]sulfate was determined by beta counting.

these four lysine residues (K_{260}, K_{262}, K_{263} and K_{264}) was subjected to analysis using site-directed mutagenesis.

Surprisingly, neither substitution of each individual lysine with alanine or leucine, nor substitution of all of them with alanine resulted in growth inhibition. Radiolabeling experiments confirmed that the mutated proteins possessed the ability to take up sulfate, albeit with significantly affected kinetics. Except of the quadruple TRAstAK$_{260\text{-}264}$A mutant, all variants of AstA with a single lysine in CCL mutated had lower transportation constants (K_t) for sulfate, which indicated enhanced affinity for sulfate. However, we did not find any similar potentially beneficial substitution in sequences of AstA orthologues from other fungi. This apparently surprising finding may be explained by AstA's ability to transport sulfite and choline sulfate ester (Holt *et al.*, 2017), which implies that under physiological conditions CCL of AstA should be flexible enough to conform to all these substrates. This versatility of AstA might also prevent substitution of K_{263} or K_{264} by a hydrophobic amino acid, which does not occur in nature. While all four single lysine substitutions into alanine resulted in the decreased maximum velocity of sulfate transport, unexpectedly, we found two substitutions among K to L mutants (K_{263}L and K_{264}L) leading to the increased velocity of transportation by 82.4 and 142%, respectively (Table 2). These changes in kinetic properties might result from enhanced CCL flexibility during MFS transporter movements. Regarding that the XylE transporter CCL forms transient latch-like structure (Wisedchaisri *et al.*, 2014), it might be difficult to verify the transient hydrophobic enzyme-substrate interactions relying solely on solid crystal structures.

Among the single amino-acid substitution mutants, TRAstA$_{262}$L had the most affected sulfate uptake rate and velocity of transportation (V_{max}). Its growth on solid minimal media was also significantly affected after 48 h, however, in a longer time TRAstA$_{262}$L reached growth rate similar to that of the wild type TRAstAWT strain. None of the K_{262} substitutions studied here altered K_t, indicating that this lysine 262 is not involved in direct interaction with the sulfate.

The quadruple TRAstAK$_{260\text{-}264}$A mutant with all four lysine residues substituted, exhibited the most visibly altered substrate transportation, which could also be observed as a decreased selenate resistance on a minimal solid medium. This result suggests that negatively charged lysine residues in wild type CCL of AstA are necessary for the maximum efficiency of the transporter. However, the quadruple $K_{260\text{-}264}$A mutation in CCL did not abolish AstA function completely, as opposed to mutations in CCL of *C. albicans* Mdr1 multidrug transporter (Mandal *et al.*, 2012). Shortening of CCL in Mdr1 eliminated the drug resistance, suggesting an important

Table 2. List of strains and plasmids

Designation	Genotype or relevant features	Reference or source
E. coli strain XL1 Blue	*recA1 endA1 gyrA96 thi-1 hsdR17 supE44 relA1 lac* [F' *proAB lacI*^{q} *ZΔM15* Tn10 (Tetr)]^c	Stratagene
A. nidulans strains		
M111	*sB43 pyrG89 pyroA4 yA2*	laboratory collection
M111 [*pyr-4*$^+$]	*sB43 pyrG89* [*Ncpyr-4*$^+$] *pyroA4 yA2*	this study
TRAstAWT M111 [*astA*$^+$, *pyr-4*$^+$]	*sB43 pyrG89* [*astA*$^+$ *Ncpyr-4*$^+$] *pyroA4 yA2*	this study
TRSBWT M111 [*sB*$^+$, *pyr-4*$^+$]	*sB43 pyrG89* [*sB*$^+$ *Ncpyr-4*$^+$] *pyroA4 yA2*	this study
TRAstAK$_{260}$A M111 [*astAK*$_{260}$A$^+$, *pyr-4*$^+$]	*sB43 pyrG89* [*astAK*$_{260}$A$^+$ *Ncpyr-4*$^+$] *pyroA4 yA2*	this study
TRAstAK$_{260}$L M111 [*astAK*$_{260}$L$^+$, *pyr-4*$^+$]	*sB43 pyrG89* [*astAK*$_{260}$L$^+$ *Ncpyr-4*$^+$] *pyroA4 yA2*	this study
TRAstAK$_{262}$A M111 [*astAK*$_{262}$A$^+$, *pyr-4*$^+$]	*sB43 pyrG89* [*astAK*$_{262}$A$^+$ *Ncpyr-4*$^+$] *pyroA4 yA2*	this study
TRAstAK$_{262}$L M111 [*astAK*$_{262}$L$^+$, *pyr-4*$^+$]	*sB43 pyrG89* [*astAK*$_{262}$L$^+$ *Ncpyr-4*$^+$] *pyroA4 yA2*	this study
TRAstAK$_{263}$A M111 [*astAK*$_{263}$A$^+$, *pyr-4*$^+$]	*sB43 pyrG89* [*astAK*$_{263}$A$^+$ *Ncpyr-4*$^+$] *pyroA4 yA2*	this study
TRAstAK$_{263}$L M111 [*astAK*$_{263}$L$^+$, *pyr-4*$^+$]	*sB43 pyrG89* [*astAK*$_{263}$L$^+$ *Ncpyr-4*$^+$] *pyroA4 yA2*	this study
TRAstAK$_{264}$A M111 [*astAK*$_{264}$A$^+$, *pyr-4*$^+$]	*sB43 pyrG89* [*astAK*$_{264}$A$^+$ *Ncpyr-4*$^+$] *pyroA4 yA2*	this study
TRAstAK$_{264}$L M111 [*astAK*$_{264}$L$^+$, *pyr-4*$^+$]	*sB43 pyrG89* [*astAK*$_{264}$L$^+$ *Ncpyr-4*$^+$] *pyroA4 yA2*	this study
TRAstAK$_{260\text{-}264}$A M111 [*astAK*$_{260\text{-}264}$A$^+$, *pyr-4*$^+$]	*sB43 pyrG89* [*astAK*$_{260\text{-}264}$A$^+$ *Ncpyr-4*$^+$] *pyroA4 yA2*	this study
TRAstAWTGFP M111 [*astA*-GFP$^+$, *pyr-4*$^+$]	*sB43 pyrG89* [*astA*-GFP$^+$ *Ncpyr-4*$^+$] *pyroA4 yA2*	this study
TRAstAK$_{260}$AGFP M111 [*astAK*$_{260}$A-GFP$^+$, *pyr-4*$^+$]	*sB43 pyrG89* [*astAK*$_{260}$A-GFP$^+$ *Ncpyr-4*$^+$] *pyroA4 yA2*	this study
TRAstAK$_{260}$LGFP M111 [*astAK*$_{260}$L-GFP$^+$, *pyr-4*$^+$]	*sB43 pyrG89* [*astAK*$_{260}$L-GFP$^+$ *Ncpyr-4*$^+$] *pyroA4 yA2*	this study
TRAstAK$_{262}$AGFP M111 [*astAK*$_{262}$A-GFP$^+$, *pyr-4*$^+$]	*sB43 pyrG89* [*astAK*$_{262}$A-GFP$^+$ *Ncpyr-4*$^+$] *pyroA4 yA2*	this study
TRAstAK$_{262}$LGFP M111 [*astAK*$_{262}$L-GFP$^+$, *pyr-4*$^+$]	*sB43 pyrG89* [*astAK*$_{262}$L-GFP$^+$ *Ncpyr-4*$^+$] *pyroA4 yA2*	this study
TRAstAK$_{263}$AGFP M111 [*astAK*$_{263}$A-GFP$^+$, *pyr-4*$^+$]	*sB43 pyrG89* [*astAK*$_{263}$A-GFP$^+$ *Ncpyr-4*$^+$] *pyroA4 yA2*	this study
TRAstAK$_{263}$LGFP M111 [*astAK*$_{263}$L-GFP$^+$, *pyr-4*$^+$]	*sB43 pyrG89* [*astAK*$_{263}$L-GFP$^+$ *Ncpyr-4*$^+$] *pyroA4 yA2*	this study
TRAstAK$_{264}$AGFP M111 [*astAK*$_{264}$A-GFP$^+$, *pyr-4*$^+$]	*sB43 pyrG89* [*astAK*$_{264}$A-GFP$^+$ *Ncpyr-4*$^+$] *pyroA4 yA2*	this study
TRAstAK$_{264}$LGFP M111 [*astAK*$_{264}$L-GFP$^+$, *pyr-4*$^+$]	*sB43 pyrG89* [*astAK*$_{264}$L-GFP$^+$ *Ncpyr-4*$^+$] *pyroA4 yA2*	this study
TRAstAK$_{260\text{-}264}$AGFP M111 [*astAK*$_{260\text{-}264}$A-GFP$^+$, *pyr-4*$^+$]	*sB43 pyrG89* [*astAK*$_{260\text{-}264}$A-GFP$^+$ *Ncpyr-4*$^+$] *pyroA4 yA2*	this study
Plasmids	description	
pBluescript KS(–)	cloning vector, Amp^r	Stratagene

HELp1	increases *A. nidulans* transformation efficiency about 200 fold	Gems & Clutterbuck 1993
kPG23B	bearing entire *N. crassa pyr-4* in pBluescript II KS(-)	laboratory collection
kPG23ΨastA	bearing Ψ*astA* pseudogene in kPG23B	this study
kPB611-12	bearing Ψ*astA* pseudogene with reconstituted 11-12TM-encoding sequence and *N. crassa pyr-4* cassette	this study
kPSB1	bearing entire *A. nidulans sB* gene in pBluescript II KS(-)	Piłsyk *et al*. 2007
kPMS11-52	BamHI-SalI insert bearing *astA* gene in pBluescript KS(–) vector	Piłsyk *et al*. 2007
kPMS11-524	kPMS11-52 with *N. crassa pyr-4* cassette ligated into PvuII site	this study
kPMS11-524K260A	kPMS11-524-derived mutated K_{260}A *astA* allele	this study
kPMS11-524K260L	kPMS11-524-derived mutated K_{260}L *astA* allele	this study
kPMS11-524K262A	kPMS11-524-derived mutated K_{262}A *astA* allele	this study
kPMS11-524K262L	kPMS11-524-derived mutated K_{262}L *astA* allele	this study
kPMS11-524K263A	kPMS11-524-derived mutated K_{263}A *astA* allele	this study
kPMS11-524K263L	kPMS11-524-derived mutated K_{263}L *astA* allele	this study
kPMS11-524K264A	kPMS11-524-derived mutated K_{264}A *astA* allele	this study
kPMS11-524K264L	kPMS11-524-derived mutated K_{264}L *astA* allele	this study
kPMS11-524K260-264A	kPMS11-524-derived mutated $K_{260\text{-}264}$A *astA* allele	this study
kPMS11-5243	kPMS11-524-derived *astA* gene fused with GFP-encoding gene	this study
kPMS11-5243K260A	kPMS11-5243-derived mutated K_{260}A *astA* allele	this study
kPMS11-5243K260L	kPMS11-5243-derived mutated K_{260}L *astA* allele	this study
kPMS11-5243K262A	kPMS11-5243-derived mutated K_{262}A *astA* allele	this study
kPMS11-5243K262L	kPMS11-5243-derived mutated K_{262}L *astA* allele	this study
kPMS11-5243K263A	kPMS11-5243-derived mutated K_{263}A *astA* allele	this study
kPMS11-5243K263L	kPMS11-5243-derived mutated K_{263}L *astA* allele	this study
kPMS11-5243K264A	kPMS11-5243-derived mutated K_{264}A *astA* allele	this study
kPMS11-5243K264L	kPMS11-5243-derived mutated K_{264}L *astA* allele	this study
kPMS11-5243K260-264A	kPMS11-5243-derived mutated $K_{260\text{-}264}$A *astA* allele	this study

role of the loop for the functioning of this transporter. Since insertional mutagenesis restoring the loop length did not result in a functional transporter, one can infer that the amino acid composition of CCL is more relevant to substrate transport than its mere length.

Altogether, our results indicate that CCL is not essential for the function of the entire transporter, but seems to be engaged in controlling of AstA activity. Interestingly, it has been found earlier that CCL of the *E. coli* lactose permease is involved in allosteric regulation by the glucose-specific enzyme IIA of the phosphoenolpyruvate: sugar phosphotransferase system (Hoischen *et al*., 1996, Seok *et al*., 1997). Similarly, CCL in the human GLUT1 transporter mediates ATP-dependent inhibition of glucose transport (Blodgett *et al*., 2007). In similar way, the AstA CCL could interact with the sulfate and form an allosteric site controlling the transporter's activity. Since AstA is ATP-independent, as we have shown (Fig. 6), fungi bearing this gene may have a higher evolutionary fitness under the low oxygen conditions, when ATP synthesis is limited, for instance in a situation of the pathogens infecting host tissue.

The findings presented by Weinglass and Kaback (2000) show that the cytoplasmic loop between helices VI and VII functions as a temporal delay spacer upon insertion of the first six helices into the translocon, and their subsequent movement into the bilayer before insertion of the last six helices. Additionally, sequence alignments of LacY CCL indicate that this region is very poorly conserved (Weinglass & Kaback, 2000). Detailed studies of *E. coli* LacY by Frillingos and coworkers (Frillingos *et al.,* 1998) and Weinglass and Kaback (Weinglass & Kaback, 2000) show that the bacterial LacY CCL plays no direct role in the substrate transportation. Bacterial MFS may be easily split into two halves discarding CCL, and the generated mutant exhibits expression and activity comparable to the wild type (Weinglass & Kaback 2000). Even an introduction of the stretches of random hydrophilic amino acid into the poorly active Δ20 aa CCL mutant, partially restores its activity, up to the 30–50% of the wild-type level. Thus, in a case of bacterial MFS transporters, CCL seems not to be particularly important for the protein function. In contrast to what was observed for the bacterial LacY transporter and its CCL, our studies indicate that AstA CCL sequence has tightly conserved length and high amino acid homology (over 70%) among numerous fungal species (Fig. 2A).

In this paper, we demonstrated that eukaryotic MFS may have different kinetics than bacterial transporters. In

contrast to *E. coli* LacY, the fungal AstA mutants: single substituted K_{260}, K_{264} or quadruple $K_{260\text{-}264}$A led to a competitive inhibition of sulfate transportation by altering K_t.

Since the lysine substitutions in CCL resulted in the altered sulfate transportation constants (K_t) in the AstA transporters, it seems likely that CCL limits the AstA affinity for substrate under the conditions of high intracellular sulfate concentration. Consequently, the substitutions of the lysine residues in CCL could abolish that allosteric regulation, resulting in an altered sulfate affinity of the mutated AstA variants. The most pronounced shift in K_t was observed for quadruple TRAstA$K_{260\text{-}264}$A mutant, which was also susceptible to selenate, a toxic analog of sulfate. Since an alteration of a substrate binding constant usually refers to a competitive inhibition of the enzyme binding site (Strelow *et al.*, 2012), our results indicate that CCL indeed interacts with the sulfate. Whether the proposed binding of sulfate by CCL would be assisted by interaction with other proteins, as it is in the case of the *E. coli* lactose permease, remains an open question.

The observed physiological effects of the mutations affecting CCL could be alternatively explained, if one assumed that CCL formed a proofreading centre (or a checkpoint), controlling the parameters of the incoming substrate. Such possibility is supported by our observation that the K_{260}A, K_{260}L, K_{263}A and K_{264}L mutants of AstA with decreased K_t (Table 2) were more resistant to selenate (Fig. 3), suggesting that these mutations could affect interaction with selenate rather than with the sulfate. Hence, CCL could be a flexible goalkeeper of the AstA transporter, forming a transient substrate-interacting pocket, acting as a checkpoint for the molecules entering the cell.

Numerous biochemical studies characterizing the MFS transporters were focused on substrate translocation pore, located within TM helices. However, K_t or K_m values are still poorly studied, and CCL has not been well investigated. The mutations introduced in substrate binding site of MFS transporters usually lead to a pronounced 10-fold K_m alteration (Will *et al.*, 1998; Sahin-Tóth *et al.*, 1999). Among some previously described enzymes, S-1,2-propanediol oxidoreductase (FucO) alters its substrate specificity substantially upon just a single point mutation L_{259}V in the substrate-binding site, while its K_m increases just two-fold (Blikstad *et al.*, 2014). In case of the higher eukaryotes, some mutated enzymes, it was shown that human galactokinase, point-mutated in its substrate-binding site (A_{198}V), has K_m only weakly altered (30% decrease) and its kinetic parameters are almost comparable to the wild type (Timson & Reece, 2003). However, the A_{198}V mutation in galactokinase is severely manifested on the cellular and organism level, with a clinical phenotype of a tendency to develop cataracts (Okano *et al.*, 2001). Since there is no data referring to kinetic parameters of eukaryotic CCL, it was not possible to compare our results to published values.

Crystal studies of the bacterial XylE transporter revealed that CCL can act as a structural linker between the N- and C-terminal domains of MFS proteins, transiently forming a latch-like structure (Wisedchaisri *et al.*, 2014). Till now, CCL was regarded as a structural linker only, but we have shown that this loop can affect the substrate uptake. Considering that some mutations located within the linker resulted in the significant K_t shifts, CCL may also participate in substrate recognition. Summarizing, the presented results suggest that the four lysine residues located within the CCL linker region are not necessary for the sulfate transport, but they select for the incoming substrate and facilitate its uptake.

Acknowledgements

We are indebted to Dr. Małgorzata Lichocka for her help in confocal microscopy and to Prof. Andrzej Paszewski for his careful reading of the manuscript. We are also indebted to Dr. Joanna Kamińska for a gift of the anti-αPma1p antibodies.

Acknowledgements od Financial Support

This work was supported by the State Committee for Scientific Research/National Center of Science (NCN), grant number N N303 814040 to S.P. and by The European Regional Development Fund and Innovative Economy, Poland, grant number UDA-POIG.01.03.01-14-038/09 to J.S.K. The equipment used was sponsored in part by the Centre for Preclinical Research and Technology (CePT), a project co-sponsored by The Innovative Economy, The National Cohesion Strategy of Poland.

REFERENCES

Abramson J, Smirnova I, Kasho V, Verner G, Kaback HR, Iwata S (2003) Structure and mechanism of the lactose permease of *Escherichia coli*. *Science* **301**: 610–615. https://doi.org/10.1126/science.1088196

Alper SL, Sharma AK (2013) The SLC26 gene family of anion transporters and channels. *Mol Aspects Med* **34**: 494–515. https://doi.org/10.1016/j.mam.2012.07.009

Altschul SF, Lipman DJ (1990) Protein database searches for multiple alignments. *Proc Natl Acad Sci* USA **87**: 5509–5513

Arst HN Jr (1968) Genetic analysis of the first steps of sulphate metabolism in *Aspergillus nidulans*. *Nature* **219**: 268–270. https://doi:10.1038/219268a0

Biswas C, Djordjevic JT, Zuo X, Boles E, Jolliffe KA, Sorrell TC, Chen SC (2013) Functional characterization of the hexose transporter Hxt13p: an efflux pump that mediates resistance to miltefosine in yeast. *Fungal Genet Biol* **61**: 23–32. https://doi.org/10.1016/j.fgb.2013.09.005

Blikstad C, Dahlström KM, Salminen TA, Widersten M (2014) Substrate scope and selectivity in offspring to an enzyme subjected to directed evolution. *FEBS J* **281**: 2387–2398. https://doi.org/10.1111/febs.12791

Blodgett DM, De Zutter JK, Levine KB, Karim P, Carruthers A (2007) Structural basis of GLUT1 inhibition by cytoplasmic ATP. *J Gen Physiol* **130**: 157–168. https://doi.org/10.1085/jgp.200709818

Bourne Y, Dannenberg J, Pollmann V, Marchot P, Pongs O (2001) Immunocytochemical localization and crystal structure of human frequenin (neuronal calcium sensor 1). *J Biol Chem* **276**: 11949–11955. https://doi.org/10.1074/jbc.M009373200

Bowler MW, Montgomery MG, Leslie AG, Walker JE (2006) How azide inhibits ATP hydrolysis by the F-ATPases. *Proc Natl Acad Sci U S A* **103**: 8646–8649. https://doi.org/10.1073/pnas.0602915103

Buchan DW, Minneci F, Nugent TC, Bryson K, Jones DT (2013). Scalable web services for the PSIPRED Protein Analysis Workbench. *Nucleic Acids Res* **41** (Web Server issue): W340-W348. https://doi.org/10.1093/nar/gkt381

Cerqueira GC, Arnaud MB, Inglis DO, Skrzypek MS, Binkley G, Simison M, Miyasato, SR, Binkley J, Orvis J, Shah P, Wymore F, Sherlock G, Wortman JR (2014). The *Aspergillus* Genome Database: multispecies curation and incorporation of RNA-Seq data to improve structural gene annotations. *Nucleic Acids Res* **42**: D705–D710. https://doi.org/10.1093/nar/gkt1029

Clutterbuck AJ (1994) Linkage map and locus list. *Prog Ind Microbiol* **29**: 791–824

Dang S, Sun L, Huang Y, Lu F, Liu Y, Gong H, Wang J, Yan N (2010) Structure of a fucose transporter in an outward-open conformation. *Nature* **467**: 734–738. https://doi.org/10.1038/nature09406

Edgar RC (2004) MUSCLE: multiple sequence alignment with high accuracy and high throughput. *Nucleic Acids Res* **32**: 1792–1797. https://doi.org/10.1093/nar/gkh340

Ethayathulla AS, Yousef MS, Amin A, Leblanc G, Kaback HR (2014) Structure-based mechanism for Na+/melibiose symport by MelB. *Nature Commun* **5**: 3009. https://doi.org/10.1038/ncomms4009

Frillingos S, Sahin-Tóth M, Wu J, Kaback HR (1998) Cys-scanning mutagenesis: a novel approach to structure function relationships in

polytopic membrane proteins. *FASEB J* **12**: 1281–1299. https://doi.org/10.1096/fasebj.12.13.1281
Gems DH, Clutterbuck AJ (1993) Co-transformation with autonomously-replicating helper plasmids facilitates gene cloning from an *Aspergillus nidulans* gene library. *Curr Genet* **24**: 520–524
Hirai T, Heymann JA, Shi D, Sarker R, Maloney PC, Subramaniam S (2002) Three-dimensional structure of a bacterial oxalate transporter. *Nat Struct Biol* **9**: 597–600. https://doi.org/10.1038/nsb821
Hofmann K, Stoffel W (1993) TMbase – A database of membrane spanning proteins segments. *Biol Chem Hoppe-Seyler* **374**: 166
Hoischen C, Levin J, Pitaknarongphorn S, Reizer J, Saier MH Jr (1996) Involvement of the central loop of the lactose permease of *Escherichia coli* in its allosteric regulation by the glucose-specific enzyme IIA of the phosphoenolpyruvate-dependent phosphotransferase system. *J Bacteriol* **178**: 6082–6086
Holt S, Kankipati H, De Graeve S, Van Zeebroeck G, Foulquié-Moreno MR, Lindgreen S, Thevelein JM (2017) Major sulfonate transporter Soa1 in *Saccharomyces cerevisiae* and considerable substrate diversity in its fungal family. *Nat Commun* **8**: 14247. https://doi.org/10.1038/ncomms14247
Iancu CV, Zamoon J, Woo SB, Aleshi, A, Choe JY (2013) Crystal structure of a glucose/H^+ symporter and its mechanism of action. *Proc Natl Acad Sci U S A* **110**: 17862–17867. https://doi.org/10.1073/pnas.1311485110
Kasahara T, Ishiguro M, Kasahara M (2006) Eight amino acid residues in transmembrane segments of yeast glucose transporter Hxt2 are required for high affinity transport. *J Biol Chem* **281**: 18532–18538. https://doi.org/10.1074/jbc.M602123200
Kasahara T, Maeda M, Bole,s E, Kasahara M (2009) Identification of a key residue determining substrate affinity in the human glucose transporter GLUT1. *Biochim Biophys Acta* **1788**: 1051–1055. https://doi.org/10.1016/j.bbamem.2009.01.014
Kertesz MA (2001) Bacterial transporters for sulfate and organosulfur compounds. *Res Microbiol* **152**: 279–290
Kuwano T, Shirataki C, Itoh Y (2008) Comparison between polyethylene glycol- and polyethylenimine-mediated transformation of *Aspergillus nidulans*. *Curr Genet* **54**: 95–103. https://doi.org/10.1007/s00294-008-0204-z
Law CJ, Maloney PC, Wang DN (2008) Ins and outs of major facilitator superfamily antiporters. *Annu Rev Microbiol* **62**: 289–305. https://doi.org/10.1146/annurev.micro.61.080706.093329
Lemieux MJ, Huan, Y, Wang DN (2004) The structural basis of substrate translocation by the *Escherichia coli* glycerol-3-phosphate transporter: a member of the major facilitator superfamily. *Curr Opin Struct Biol* **14**: 405–412. https://doi.org/10.1016/j.sbi.2004.06.003
Letunic I, Bork P (2017) 20 years of the SMART protein domain annotation resource. *Nucleic Acids Res* **46**(D1): D493–D496. https://doi:10.1093/nar/gkx922
Lowry OH, Rosebrough NJ, Farr AL, Randall RJ (1951) Protein measurement with the Folin phenol reagent. *J Biol Chem* **193**: 265–275
Łukaszkiewicz Z, Paszewski A (1976) Hyper-repressible operator-type mutant in sulphate permease gene of *Aspergillus nidulans*. *Nature* **259**: 337–338. https://doi.org/10.1038/259337a0
Mandal A, Kumar A, Singh A, Lynn AM, Kapoor K, Prasad R (2012) A key structural domain of the *Candida albicans* Mdr1 protein. *Biochem J* **445**: 313–322. https://doi.org/10.1042/BJ20120190
Martinelli SD (1994) Gene symbols. *Prog Ind Microbiol* **29**: 825–827
Okano Y, Asada M, Fujimoto A, Ohtake A, Murayama K, Hsiao KJ, Choeh K, Yang Y, Cao Q, Reichardt JK, Niihira S, Imamura T, Yamano T (2001) A genetic factorfor age-related cataract: identification and characterization of a novel galactokinase variant, 'Osaka', in Asians. *Am J Hum Genet* **68**: 1036–1042. https://doi.org/10.1086/319512
Pasrija R, Banerjee D, Prasad R (2007) Structure and function analysis of CaMdr1p, a major facilitator superfamily antifungal efflux transporter protein of *Candida albicans*: identification of amino acid residues critical for drug/H+ transport. *Eukaryot Cell* **6**: 443–453. https://doi.org/10.1128/EC.00315-06
Patron M, Checchetto V, Raffaello A, Teardo E, Reane DV, Mantoan M, Granatiero V, Szabo I, De Stefani D, Rizzuto R (2014) MICU1 and MICU2 finely tune the mitochondrial Ca^{2+} uniporter by exerting opposite effects on MCU activity. *Mol Cell* **53**: 726–737. https://doi.org/10.1016/j.molcel.2014.01.013
Paulsen IT, Brown MH, Skurray RA (1996) Proton-dependent multidrug efflux systems. *Microbiol Rev* **60**: 575–608
Pedersen BP, Kumar H, Waight AB, Risenmay AJ, Roe-Zurz, Z., Chau BH, Schlessinger A, Bonomi M, Harries W, Sali A, Johri AK, Stroud RM (2013) Crystal structure of a eukaryotic phosphate transporter. *Nature* **496**: 533–536. https://doi.org/10.1038/nature12042
Piłsyk S, Natorff R, Sieńko M, Paszewski A (2007) Sulfate transport in *Aspergillus nidulans*: a novel gene encoding alternative sulfate transporter. *Fungal Genet Biol* **44**: 715–725. *https://doi.org/10.1016/j.fgb.2006.11.007*
Piłsyk S, Paszewski A (2009) Sulfate permeases – phylogenetic diversity of sulfate transport. *Acta Biochim Pol* **56**: 375–384
Piłsyk S, Natorff R, Gawińska-Urbanowicz H, Kruszewska JS (2015) *Fusarium sambucinum astA* gene expressed during potato infection is a functional orthologue of *Aspergillus nidulans astA*. *Fungal Biol* **119**: 509–517. https://doi.org/10.1016/j.funbio.2015.02.002
Rost B, Yachdav G, Liu J (2004) The PredictProtein Server. *Nucleic Acids Res* **32** (Web Server issue): W321–W326. https://doi.org/10.1093/nar/gkh377
Roth V (2006) Doubling Time Computing, Available from: http://www.doubling-time.com/compute.php
Roy A, Kucukural A, Zhang Y (2010) I-TASSER: a unified platform for automated protein structure and function prediction. *Nature Protocols* **5**: 725–738. https://doi.org/10.1038/nprot.2010.5
Roy A, Yang J, Zhang, Y (2012) COFACTOR: an accurate comparative algorithm for structure-based protein function annotation. *Nucleic Acids Res* **40** (Web Server issue): W471-7. https://doi.org/10.1093/nar/gks372
Sahin-Tóth M, le Coutre J, Kharabi D, le Maire G, Lee JC, Kaback HR (1999) Characterization of Glu126 and Arg144, two residues that are indispensable for substrate binding in the lactose permease of *Escherichia coli*. *Biochemistry* **38**: 813–819. https://doi.org/10.1021/bi982200h
Sambrook J, Fritsch EF, Maniatis T (1989) Molecular cloning: a laboratory manual. *Cold Spring Harbor Laboratory Press*. https://doi.org/10.1016/0092-8674(90)90210-6
Sayle RA, Milner-White EJ (1995) RASMOL: biomolecular graphics for all. *Trends Biochem Sci* **20**: 374. https://doi.org/10.1016/S0968-0004(00)89080-5
Seok YJ, Sun J, Kaback HR, Peterkofsky A (1997) Topology of allosteric regulation of lactose permease. *Proc Natl Acad Sci U S A* **94**: 13515–13519. https://doi.org/10.1073/pnas.94.25.13515
Sieńko M, Natorff R, Skoneczny M, Kruszewska J, Paszewski A, Brzywczy J (2014) Regulatory mutations affecting sulfur metabolism induce environmental stress response in *Aspergillus nidulans*. *Fungal Genet Biol* **65**: 37–47. https://doi.org/10.1016/j.fgb.2014.02.001
Strelow J, Dewe W, Iversen PW, Brooks HB, Radding JA, McGee J, Weidner J (2012) Mechanism of Action Assays for Enzymes, In *Assay Guidance Manual*, Sittampalam GS, Coussens NP, Nelson H *et al*, eds, Eli Lilly & Company and the National Center for Advancing Translational Sciences, 2004
Sun L, Zeng X, Yan C, Sun X, Gong X, Rao Y, Yan N (2012) Crystal structure of a bacterial homologue of glucose transporters GLUT1-4. *Nature* **490**: 361–366. https://doi.org/10.1038/nature11524
Timson DJ, Reece RJ (2003) Functional analysis of disease-causing mutations in human galactokinase. *Eur J Biochem* **270**: 1767–1774. https://doi.org/10.1046/j.1432-1033.2003.03538.x
Tweedie JW Segel IH (1970) Specificity of transport processes for sulfur, selenium, and molybdenum anions by filamentous fungi. *Biochim Biophys Acta* **196**: 95–106. https://doi.org/10.1016/0005-2736(70)90170-7
Weinglass AB, Kaback HR (2000) The central cytoplasmic loop of the major facilitator superfamily of transport proteins governs efficient membrane insertion. *Proc Natl Acad Sci U S A* **97**: 8938–8943. https://doi.org/10.1073/pnas.140224497
Will A, Grassl R, Erdmenger J, Caspari T, Tanner W (1998) Alteration of substrate affinities and specificities of the *Chlorella* Hexose/H+ symporters by mutations and construction of chimeras. *J Biol Chem* **273**: 11456–11462. https://doi.org/10.1074/jbc.273.19.11456
Wisedchaisri G, Park MS, Iadanza MG, Zhen H, Gonen T (2014) Proton-coupled sugar transport in the prototypical major facilitator superfamily protein XylE. *Nat Commun* **5**: 4521. https://doi.org/10.1038/ncomms5521
Woodin TS Wang JL (1989) Sulfate permease of *Penicillium duponti*. Exp Mycol **13**:380-391. https://doi.org/10.1016/0147-5975(89)90034-0
Yin Y, He X, Szewczyk P, Nguyen T, Chang G (2006) Structure of the multidrug transporter EmrD from *Escherichia coli*. *Science* **312**: 741–744. https://doi.org/10.1126/science.1125629
Zhang Y (2008) I-TASSER server for protein 3D structure prediction. *BMC Bioinformatics* **9**: 40. https://doi.org/10.1186/1471-2105-9-40